Torque vectoring control of an electric vehicle with in-wheel motors

Nuno Alexandre de Almeida Salgueiro
nuno.salgueiro@tecnico.ulisboa.pt
Instituto Superior Técnico

***Abstract*—Optimal torque distribution of the driving wheels of a vehicle is an open problem. Currently solved with a mechanical differential, nowadays with the electric engine and in particular with an engine per wheel, there is room for other solutions. We rewrite the problem of "how to turn fast without sliding" taking into account the traction control, developing a system with a starting point and endpoint being the four wheels and the traction with four wheels, and how that model may help estimate and control a vehicle in such a way that you have better performance and handling. Beyond the mathematical model based on the LuGre tire model, an observer and controller were developed as a Kalman Filter and a Model Predictive controller, as a proof of concept with the observer being validated with real data of a Formula Student car, FST09e. We therefore conclude that the approach here taken is valid, that the equations within properly represent the dynamics of the vehicle attitude and that a controller capable of taking into account power constraints, traction, lateral stability and desired yaw rate is possible.**

***Index Terms*—Torque Vectoring, Kalman Filter, Model Predictive Control, LuGre, State-Space**

I. Introduction

The Torque Vectoring problem has been present in the automotive industry for quite some time. The electric car, and the electric engine has brought new avenues of research and problems. With an electric engine per wheel, the usual mechanical differential could no longer be employed but the freedom of actuation brought new opportunities. The work presented here started in the Formula Student Lisboa with a simple controller for torque distribution and the lack of a proper controller for the team provided the motivation for this work.

Torque Vectoring is about finding an answer to the problem of "how fast can I turn without slipping?" by controlling the driving/braking torque at each wheel. In respect to the electric car it became evident that, with an electric engine, the deadzone of actuation (previously only with brakes) in respect to the roll steer effect could be further reduced when compared to the traditional combustion engine car (Folke 2010) [20]. Yaw rate control was to be the primary aim of this system and a controller was made [20] with feedforward, based on a set-point operation.

The actual impacts of an all electric car, beyond the ecological scope, were surmised (DeNovellis 2012) [40]. Not just the roll stability, but the handling, directional stability, energy consumption, braking/traction (lateral/longitudinal dynamics) and attitude control and road-holding (vertical dynamics) could be affected.

By 2012, the state-of-the art could be said to be the E-VECTOORC [10] project for a 4 wheel(4WD) electric car. Noteworthy is the approach used to estimate the friction conditions with the electric engine, instead of with the hydraulic brake pressure and the slip ratio controller. Beyond that, the main objectives of this project were the extension of the linear region in respect to wheel steer δ and lateral acceleration a_y - more steering angle, more lateral acceleration in a linear relationship, and minimizing the impact of emergency manoeuvres to the vehicle heading.

Since then, other approaches have been made. To name a few: with a focus on the lane changing problem and an explicit objective to replace the ABS and ESC systems [47] by considering the system as a bicycle model with load transfers, for state variables yaw rate ω_z and sideslip angle β, and for inputs the wheel steering angle and yaw moment. They also took into account the engine limitations, in respect to torque rate of change [49]. Robust approaches were also made like in [30] and [1] with the single track equations and an emphasis on the frequency response of the system.

It should be noted that although it seems to be a torque distribution problem, it is in fact a power distribution problem. Often the engines place local constraints on the power available for each wheel, and there are global constraints due to the total available power at the vehicle. The work done on this thesis attempts to write all of these constrains/requirements in such a way that the resulting solution is the torque to be applied at each wheel. The current state of the art is derived from the bicycle model, with the controller outputing a yaw moment that then needs to be translated into a torque for each wheel. Thus neglecting the available power/maximum torque constraint, the traction control problem and the lateral stability.

Our contribution lies in a slight modification to the LuGre tire model and in the derivation of a four wheel car model, resulting in a system with proven observability properties. This allowed for the development of an observer and controller, that showcases the potenciality of this approach. The controller managed to take into account the desired yaw rate, available power, the lateral stability and the traction control problem. The problem formulation here described also allows for further work in extending the controller taking into account engine temperature and wear. Also, the observer results - that require common sensors - are of particular note, since by knowing the sideslip angle β and the corresponding velocity vector, other controllers for active suspension can be done without the need of dedicated sensors, not currently available for the Formula

Student Lisboa team.

II. System Analysis

In this section we develop the mathematical model for the car dynamics. The car can be thought of as a mass with four points where force is applied to the car as $\mathbf{F}^{Car} = \sum F_i$, and with dynamics taking into account the point of application $\mathbf{r}$ of this force - tire location, and the self-aligning moment of each tire, $\sum M_{z_i} + \sum \mathbf{r}_i \times \mathbf{F}_i$. These four points are at the centre of the tire contact patches. The model that describes the tire-road interaction is called a tire model. We will start at the tire level, from the engine torque and work towards the complete car model. Starting with the single tire, a theoretical one wheeled car, to the full car model. By not taking into account any other forms of friction, we can also derive the "coasting" car and define the equilibrium points of the model.

The approach taken here to model the car behaviour is to consider the car dynamics in a 2D frame, and add the vertical dynamics, such as the load transfer, as variations of the normal load - the normal force generated at the contact patch.

Some assumptions were made about the car model. We assume that there is no camber angle (side tilt of the wheel), the road is flat, the centre of gravity is known, yaw rate and wheel turning speed are measurable in the car frame, the normal load at each tyre can be estimated, from a suspension model, and that the measured acceleration is seen from a inertial observer aligned with the car frame. This last one will be achieved with an Attitude and Heading Reference System, that removes the effect of the imaginary forces - euler, coriolis and centrifuge.

A. Tire Model

The tire model is the building block from which the car model is derived. In a 2D frame, the tire is reduced to a point that generates a force and a self-aligning torque - due to the rolling motion of the tire. The generated force, depends on the slip and how the tire is aligned in relation to the road plane(e.g. camber angle). The goal of a tire model is not only to accurately model the dynamics of the friction, sliding and the elastic deformations but also take into account how the inputs affect this.

About tire models in general, it is though that a force is generated if there is a slip between the tire and the road, given non-zero friction. This slip is called the slip ratio and is defined as

$$k = \left(\frac{\omega r}{v} - 1\right), \tag{1}$$

according to the Society of Automotive Engineers Vehicle Dynamics Standards Committee.

The angle of the velocity vector at the tire contact patch, also called the slip angle, is defined as

$$\alpha = -\arctan\left(\frac{v_y}{|v_x|}\right), \tag{2}$$

for each tire.

Most tire models agree that there is a linear relationship between the slip and the generated force, with a saturation zone where the slip is high enough that little to no force is generated at the tire.

B. LuGre Tire Model

This work is based on the LuGre dynamic tire model [7], first developed in 1995 by researchers from the universities of Lund and Grenoble and consists on an extension of the Dahl model by adding the Stribeck effect and a variable Coulomb friction force. Since then the LuGre tire model has seen more development by Tsiotras, Velenis and Sorine [56] in 2004 with the development of an exact lumped model. They also derived an approximate tire model assuming uniform load distribution of the weight along the contact patch of the tire. It is this model that is used in this thesis. This assumption results in the loss of the self-aligning torque of the tire. The work of Deur et al [13] in 2005 should also be mentioned since it further extends the model to consider camber, carcass compliance, conicity, ply steer and an additional rolling resistance term.

This model is a dynamic model that attempts to describe the tire-road interaction from a physics point of view. Here the rolling resistance is explained by the hysteresis of the model. While not as explicit as the "Magic Formula" model, this model also has a linear region in respect to the slip and, since it does not rely on an explicit ratio, is well defined at low speeds. However the self-aligning moment is not as accurate.

According to the LuGre tire model, the tire can be seen as a group of bristles that deform as they enter the contact patch of the tire. These imaginary bristles exist both in the longitudinal x and lateral y axis. The deformation z_i, with i being either x or y, is a function of the relative velocity v_{ri} of the bristle elements and the wheel angular velocity ω.

The LuGre tire model [56] is defined as,

$$\frac{dz_i(t,\zeta)}{dt} = \frac{\partial z_i(t,\zeta)}{\partial t} + |\omega r|\frac{\partial z_i(t,\zeta)}{\partial \zeta} \tag{3}$$

$$= v_{ri}(t) - C_{0i}(v_r) z_i(t,\zeta) \tag{4}$$

$$\mu_i(t,\zeta) = -\sigma_{0i} z_i(t,\zeta) - \sigma_{1i}\frac{\partial z_i(t,\zeta)}{\partial t} - \sigma_{2i} v_{ri}(t) \tag{5}$$

$$F_i(t) = \int_0^L \mu_i(t,\zeta) f_n(\zeta) d\zeta \tag{6}$$

$$M_z(t) = -\int_0^L \mu_y(t,\zeta) f_n(\zeta)\left(\frac{L}{2} - \zeta\right) d\zeta, \;\; i = x, y \tag{7}$$

with: $z_i(t,\zeta)$ as the internal friction states at time t and position ζ along the contact patch, ω is the wheel angular velocity and r the tire radius, with L the contact patch length of the tire; σ_{0i} the tire bristle stiffness with the corresponding stiction and viscous damping constants σ_{1i} and σ_{2i} of the friction coefficients $\mu_i(t,\zeta)$ and v_{ri} the relative velocity of the contact patch elements in the tire.

Thus equation 6 models the longitudinal force F_x, side force F_y and 7 the self-aligning moment M_z of the tire.

Deur [12] provided a simplified tire model by assuming a uniform load F_n at the contact patch and making some assumptions about the transient response. It was shown [56] that with a high enough stiffness the transient behaviour is a

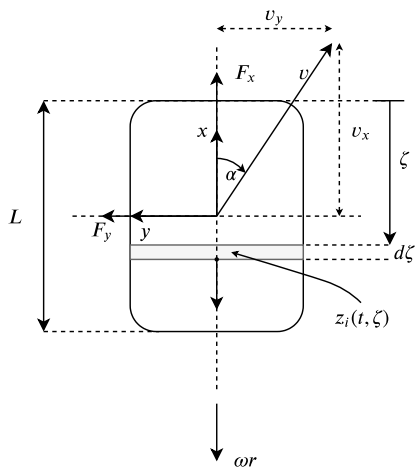

Fig. 1. Frame of reference for the LuGre tire model, in a top-down view of a tire, in the tire frame.

good approximation. This model is defined as,

$$\dot{\tilde{z}}_i(t) = v_{ri} - \left(\frac{||v_r||\sigma_{0i}}{g(v_r)} + \frac{k_i^{ss}}{L}|\omega r|\right)\tilde{z}_i \tag{8}$$

$$F_i(t) = F_n\left(\sigma_{0i}\tilde{z}_i + \sigma_{1i}\dot{\tilde{z}}_i + \sigma_{2i}v_{ri}\right) \tag{9}$$

with,

$$g(v_r) = \frac{\|M_k^2 v_r\|}{\|M_k v_r\|} + \left(\mu_s - \frac{\|M_k^2 v_r\|}{\|M_k v_r\|}\right)e^{-\left(\frac{||v_r||}{v_s}\right)^\gamma} \tag{10}$$

$$M_k = \begin{bmatrix}\mu_{kx} & 0\\ 0 & \mu_{ky}\end{bmatrix} \tag{11}$$

$$k_i^{ss} = \frac{1-e^{-L/Z_i}}{1-\frac{L}{Z_i}\left(1-e^{-L/Z_i}\right)}, Z_i = \frac{|\omega r|g(v_r)}{||vr||\sigma_{0i}} \tag{12}$$

$$v_r = \begin{bmatrix}v_{rx}\\ v_{ry}\end{bmatrix} = \begin{bmatrix}\omega r\\ 0\end{bmatrix} - \begin{bmatrix}v_x\\ v_y\end{bmatrix} \tag{13}$$

$$g(0) = \mu_s \tag{14}$$

$$i = x, y.$$

The trade-off with this approach is that the uniform load assumption results in the loss of the self-aligning moment. Usually the self-aligning moment is very small and thus this loss was deemed acceptable. In 8 k_i^{ss} is used to match the steady state behaviour of the tire and $g(v_r)$ is a function that estimates the friction, given the relative velocity of the contact patches, as a value between the static μ_s and kinetic μ_k Coulomb friction coefficients. The Stribeck velocity v_s and the shape parameter are used to model the transition from one coefficient to another in order to achieve the desired steady-state behaviour of the tire friction[12]. With this, $\tilde{z}_i$ becomes the average tire deflection in x and y.

While Velenis [58] started by defining the Coulomb friction coefficient as depending on the direction of the relative velocity vector v_r, and later reformulated the problem using only scalars, here 10, we allow for the kinetic friction to depend on the direction of the relative velocity. The only constraint that we placed on his original formulation was that it had to be continuous and the limit at (0,0) be defined.

The only way for the limit,

$$\lim_{(vr_x,vr_y)\to(0,0)} \frac{\|M_k^2 v_r\|}{\|M_k v_r\|} + \left(\frac{\|M_s^2 v_r\|}{\|M_s v_r\|} - \frac{\|M_k^2 v_r\|}{\|M_k v_r\|}\right)e^{-\left(\frac{||v_r||}{v_s}\right)^\gamma} \tag{15}$$

to be defined and allow for a continuous extension of $g(v_r)$ is for the static friction M_s to be the same along the x and y axis. Otherwise the static friction coefficient would depend on the direction of the measurement.

As such, we took the middle ground between the original definition of [58] and the final form of the LuGre tire model. With $M_s = \begin{bmatrix}\mu_s & 0\\ 0 & \mu_s\end{bmatrix}$, $g(vr)$ takes the form presented in 10 and the limit defined as,

$$\lim_{(v_{rx},v_{ry})\to(0,0)} g(v_r) = \mu_s. \tag{16}$$

The level curves of the friction coefficient, as a function of the relative velocity, for the tire configurations in this thesis can be seen in figure 2.

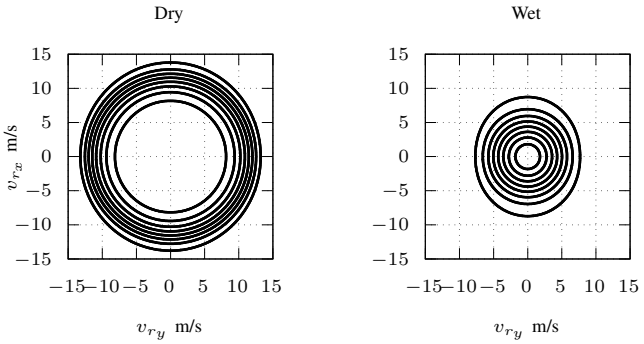

Fig. 2. $g(v_r)$ level curves as a function of the relative velocity vector v_r.

C. Linearized Tire Model

Our proposal is to take this model 17 and introduce parameters such that,

$$\dot{\tilde{z}}_i(t) = v_{ri} - O_i\tilde{z}_i \tag{17}$$

$$F_i(t) = F_n O_{\sigma i}\tilde{z}_i + F_n\sigma_i v_{ri} \tag{18}$$

with,

$$O_i = \left(\frac{||v_r||\sigma_{0i}}{g(v_r)} + \frac{k_i^{ss}}{L}|\omega r|\right) \tag{19}$$

$$O_{\sigma i} = \sigma_{0i} - \sigma_{1i}O_i \tag{20}$$

$$\sigma_i = \sigma_{1i} + \sigma_{2i}. \tag{21}$$

This linearization is done by introducing the parameters O_i and $O_{\sigma i}$, which we will call the rate of bristle restitution s^{-1} and the normalized stiffness in m^{-1}. They are assumed constant for the controller, thus disregarding the partial derivative of these terms, however the plant will have the non-linear behaviour. This approximation is equivalent to assume that

we are operating in the linear region, that we are not unduly sliding, which and can be seem in figure 3.

This allows for a linear system realization and we can use this in the model predictive part of the controller and to study the dynamics of the car (at steady-state those parameters will be constant). The new damping constant is now σ_i. It can be seen 18 that the force is proportional to the load and the bristle deflection. Another way to look at it is by comparing it to a variable stiffness spring.

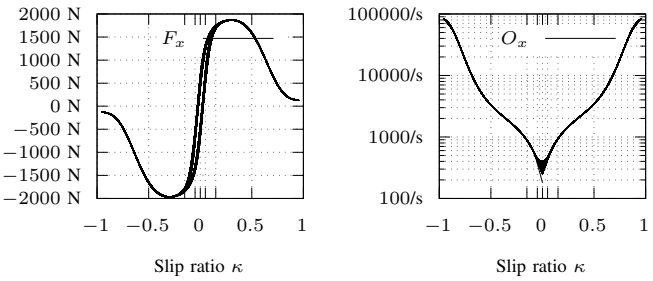

Fig. 3. Hysteresis and O_x variation with slip. Fixed velocity at 15 m/s, slip angle $\alpha = 0$ and variable wheel angular velocity triangular sweeps at 2Hz.

To the previous model we add the input wheel torque u from the engine, take into account the wheel moment of inertia I_ω and say that the input torque must overcome the corresponding generated force as,

$$I_\omega \dot{\omega} = u - rF_x \tag{22}$$

$$= u - rF_n O_{\sigma x} \tilde{z}_x - rF_n \sigma_x v_{rx}. \tag{23}$$

The linearised state-space model with states, tire deflection, wheel rotation speed and linear velocity in the tire frame can be written as,

$$\begin{bmatrix} \dot{\tilde{z}}_x \\ \dot{\tilde{z}}_y \\ \dot{\omega} \\ \dot{v}_x \\ \dot{v}_y \end{bmatrix} = \begin{bmatrix} -O_x, & 0, & r, & -1, & 0 \\ 0, & -O_y, & 0, & 0, & -1 \\ -\frac{rF_n}{I_\omega} O_{\sigma x}, & 0, & -\frac{r^2 F_n \sigma_x}{I_\omega}, & \frac{rF_n \sigma_x}{I_\omega}, & 0 \\ \frac{F_n}{m} O_{\sigma x}, & 0, & \frac{\sigma_x}{m} r, & -\frac{\sigma_x}{m}, & 0 \\ 0, & \frac{F_n}{m} O_{\sigma y}, & 0, & 0, & -\frac{\sigma_y}{m} \end{bmatrix} \begin{bmatrix} \tilde{z}_x \\ \tilde{z}_y \\ \omega \\ v_x \\ v_y \end{bmatrix} + \begin{bmatrix} 0 \\ 0 \\ \frac{1}{I_\omega} \\ 0 \\ 0 \end{bmatrix} u \tag{24}$$

The tire generates a force at the contact patch depending on the tire slip ratio κ and the slip angle α.

We estimated the LuGre tire model from the FSAE Tire Test Consortium data for the Hoosier 18.0 × 7.5 10 R25B tire, and then we modified the values to simulate not so optimum conditions, and called that tire the ”wet” tire. The estimated tire is reported in this work as the ”dry” tire. Figure 4 shows this relationship.

Assuming that everything else remains constant, the force along the y axis is most influenced by the slip angle α, while the slip ratio κ affects mostly the x axis. Both have a linear region about the origin that saturates at higher values. Furthermore, these curves can have hysteresis which is the main contributing factor to the rolling resistance.

The normal load F_n or normal force also contributes to the generated force in a linear relationship, as previously seen in the equations.

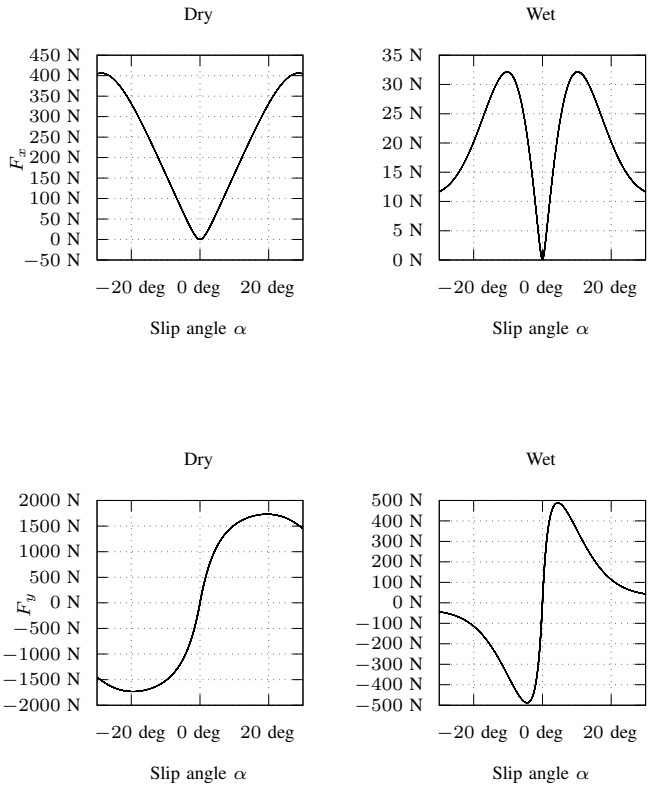

Fig. 4. Effect of tire velocity angle α on the force generated at the contact patch with fixed velocity at 15 m/s and variable α at 0.1Hz.

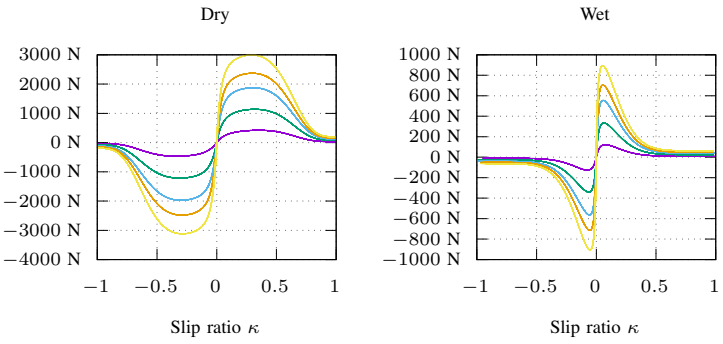

Fig. 5. Effect of normal load F_n in the force to slip ratio relationship with fixed velocity at 15 m/s, velocity angle $\alpha = 0$ and variable wheel angular velocity triangular sweeps at 0.1Hz. F_n increases from 200,500,800,1000,1250N

D. Car Model

The car model is derived from the tire model. The current state of the art consists on defining the car model as a bicycle model and defines the states as the yaw rate and the yaw moment. We took a diferent approach and deduced the car dynamics through the previous LuGre tire model for the whole car.

1) One Wheel Car: We start by studying an hypothetical car with just one wheel. This model will be the basis for the four wheel car model. The challenge here is to derive the equations in respect to the car frame and not the tire frame. To this effect we will define a linear transformation that achieves this.

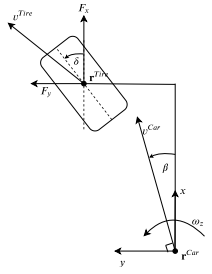

Fig. 6. Hypothetical single tire car.

Since we are assuming that the car is a rigid body, then by definition the angular velocity must be the same at all points, and beginning by assuming that there is no steering $\delta = 0$, the following must hold,

$$\mathbf{v}^{Tire} = \left[\mathbf{v}^{Car} + \boldsymbol{\omega} \times (\mathbf{r}_{Tire} - \mathbf{r}_{Car})\right]. \tag{25}$$

Further assuming that the car centre of gravity is the origin, $\mathbf{r}_{Car} = [0,0,0]^T$ and considering only planar motion with yaw rate ω_z then the velocity at the tire can be deduced as,

$$\begin{bmatrix} v_x \\ v_y \end{bmatrix}^{Tire} = \left(\begin{bmatrix} v_x \\ v_y \end{bmatrix}^{Car} + \begin{bmatrix} -r_y\omega_z \\ r_x\omega_z \end{bmatrix} \right). \tag{26}$$

To account for the steering $\delta \neq 0$ we simply have to add a rotation matrix R_δ^T to shift the orientation of the projected vector,

$$\begin{bmatrix} v_x \\ v_y \end{bmatrix}^{Tire} = R_\delta^T \left(\begin{bmatrix} v_x \\ v_y \end{bmatrix}^{Car} + \begin{bmatrix} -r_y\omega_z \\ r_x\omega_z \end{bmatrix} \right) \tag{27}$$

$$= \begin{bmatrix} \cos\delta, & \sin\delta, & r_x\sin\delta - r_y\cos\delta \\ -\sin\delta, & \cos\delta, & r_x\cos\delta + r_y\sin\delta \end{bmatrix} \begin{bmatrix} v_x^{Car} \\ v_y^{Car} \\ \omega_z \end{bmatrix} \tag{28}$$

with,

$$R_\delta = \begin{bmatrix} \cos\delta, & -\sin\delta \\ \sin\delta, & \cos\delta \end{bmatrix},$$

and we have a linear relationship between the two velocity vectors, assuming that the steering is constant.

Writing the autonomous system, using a state vector in respect to the car frame:

$$\begin{bmatrix} \dot{\tilde{z}}_x \\ \dot{\tilde{z}}_y \\ \dot{\omega} \\ \dot{v}_x \\ \dot{v}_y \\ \dot{\omega}_z \end{bmatrix} = A \begin{bmatrix} \tilde{z}_x \\ \tilde{z}_y \\ \omega \\ v_x \\ v_y \\ \omega_z \end{bmatrix}, \; A = \left[\begin{array}{c|c} A_{11} & A_{12} \\ \hline A_{21} & A_{22}, \end{array}\right] \tag{29}$$

with the block matrices $A_{11},\ A_{12}, A_{21}, A_{22}$ defined as,

$$A_{11} = \begin{bmatrix} -O_x, & 0, & r \\ 0, & -O_y, & 0 \\ -\frac{F_n r}{I_\omega} O_{\sigma x}, & 0, & \frac{-F_n r^2}{I_\omega}\sigma_x \end{bmatrix} \tag{30}$$

$$A_{12} = \begin{bmatrix} -c, & -s, & r_y c - r_x s \\ s, & -c, & -r_y s - r_x c \\ \frac{F_n r}{I_\omega}\sigma_x c, & \frac{F_n r}{I_\omega}\sigma_x s, & \frac{-F_n r}{I_\omega}\sigma_x\left(r_y c - r_x s\right) \end{bmatrix} \tag{31}$$

$$A_{21} = \begin{bmatrix} \frac{F_n}{m} O_{\sigma x} c, & -\frac{F_n}{m} O_{\sigma y} s, & \frac{F_n}{m} r\sigma_x c \\ \frac{F_n}{m} O_{\sigma x} s, & \frac{F_n}{m} O_{\sigma y} c, & \frac{F_n}{m} r\sigma_x s \\ \frac{F_n}{I_z} O_{\sigma y}(r_x s - r_y c), & \frac{F_n}{I_z} O_{\sigma y}(r_x c + r_y s), & \frac{F_n r}{I_z}\sigma_x(r_x s - r_y c) \end{bmatrix} \tag{32}$$

$$A_{22} = \begin{bmatrix} -\frac{F_n}{m}(c^2\sigma_x + s^2\sigma_y), & \frac{F_n}{m}(\sigma_y cs - \sigma_x cs), & \frac{F_n}{m}\sigma_x(r_y c^2 - r_x cs) + \frac{F_n}{m}\sigma_y(r_y c^2 + r_x cs) \\ \frac{F_n}{m}(\sigma_y cs - \sigma_x cs), & -\frac{F_n}{m}(c^2\sigma_y + s^2\sigma_x), & \frac{F_n}{m}\sigma_x s(r_y c - r_x s) - \frac{F_n}{m}\sigma_y c(r_x c + r_y s) \\ \frac{F_n}{I_z}\left[\sigma_x(r_y c^2 - r_x cs) + \sigma_y(r_y s^2 + r_x cs)\right], & \frac{F_n}{I_z}\left[\sigma_x(r_y cs - r_x s^2) - \sigma_y(r_x c^2 + r_y cs)\right], & -\frac{F_n}{I_z}\left[\sigma_x(r_y c - r_x s)^2 + \sigma_y(r_y s + r_x c)^2\right] \end{bmatrix} \tag{33}$$

$$s = \sin\delta, \; c = \cos\delta, \tag{34}$$

we define the building block of the four wheel car model.

This model has six states, three internal states - the deflections $\tilde{z}_x$, $\tilde{z}_y$ and wheel velocity ω, and three external states - car linear velocity and the yaw rate ω_z. The matrix A_{11} describes the dynamics of the internal states, and A_{22} the dynamics of the external states. A_{12} and A_{21} define the dynamics between the external and internal states.

The model outputs are the angular wheel velocity, the velocity derivatives along x and y and the yaw rate ω_z. All of them are assumed to be measurable,

$$\mathbf{y} = C\mathbf{x}, \text{with } C \in \mathbb{R}^{4\times 6} \tag{35}$$

$$= \left[\omega, \dot{v}_x, \dot{v}_y, \omega_z\right]^T. \tag{36}$$

One of the goals of this thesis was to develop an observer for the velocity vector in the car frame. For this model we were able to prove that it is observable with just these outputs.

With the observability matrix as,

$$\text{obsv} = \begin{bmatrix} C \\ CA \\ CA^2 \\ \vdots \\ CA^5 \end{bmatrix}, \tag{37}$$

we were able to confirm with the MATLAB symbolic toolbox that the rank of the observability matrix is six, which proves that all states are observable, for any steering angle and damping coefficients (including 0).

2) Four wheel Car: Using the previous model to each wheel and taking into account that the external states are shared between wheels, the four wheel car model can be derived.

Let each tire be referenced as rear right (rr), rear left (rl), front right (fr), front left (fl), then the four wheel car is

defined as,

$$\dot{\mathbf{x}} = \begin{bmatrix} A(\delta_{rr})^{rr}_{11}, & 0, & 0, & 0, & A(\delta_{rr})^{rr}_{12} \\ 0, & A(\delta_{rl})^{rl}_{11}, & 0, & 0, & A(\delta_{rl})^{rl}_{12} \\ 0, & 0, & A(\delta_{fr})^{fr}_{11}, & 0, & A(\delta_{fr})^{fr}_{12} \\ 0, & 0, & 0, & A(\delta_{fl})^{fl}_{11}, & A(\delta_{fl})^{fl}_{12} \\ A(\delta_{rr})^{rr}_{21}, & A(\delta_{rl})^{rl}_{21}, & A(\delta_{fr})^{fr}_{21}, & A(\delta_{fl})^{fl}_{21}, & \sum A_{22} \end{bmatrix} \mathbf{x} + B\mathbf{u} \quad (38)$$

$$= A(\delta_{rr}, \delta_{rl}, \delta_{fr}, \delta_{fl})\mathbf{x} + B\mathbf{u} \quad (39)$$

$$\mathbf{y} = C(\delta_{rr}, \delta_{rl}, \delta_{fr}, \delta_{fl})\mathbf{x} = \begin{bmatrix} \omega_{rr} & \omega_{rl} & \omega_{fr} & \omega_{fl} & \dot{v}_x & \dot{v}_y & \omega_z \end{bmatrix}^T \quad (40)$$

with state and input,

$$\mathbf{x} = \begin{bmatrix} z^{rr}_x, z^{rr}_y, \omega^{rr}, z^{rl}_x, z^{rl}_y, \omega^{rl}, z^{fr}_x, z^{fr}_y, \omega^{fr}, z^{fl}_x, z^{fl}_y, \omega^{fl}, v_x, v_y, \omega_z \end{bmatrix}^T \quad (41)$$

$$\mathbf{u} = \begin{bmatrix} u^{rr}, u^{rl}, u^{fr}, u^{fl} \end{bmatrix}^T. \quad (42)$$

3) Steering: In this section we describe the steering scheme that is assumed to be adopted. We assume that the car has Ackerman steering.

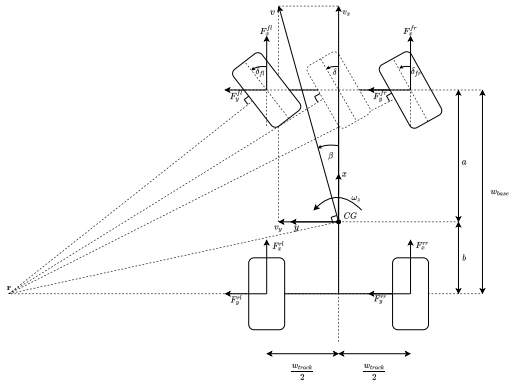

Fig. 7. Full car model assuming Ackerman steering. An imaginary wheel (equivalent to the bicycle model) turned δ rad is assumed to be controlled by the driver. This corresponds to the front right δ_{fr} and front left δ_{fl} turning angles. The wheelbase w_{base} and wheel track w_{track} are also represented. The car is assumed to have neutral steering when the turning point is on the rear axle axis, as shown in the figure. Different steering schemes can have this point closer or further away from the car.

From figure 7 and by assuming a turning point $\mathbf{r} = (r_x, r_y)$ we derive the relationship between each wheel,

$$\begin{bmatrix} \cot\delta_{fr} \\ \cot\delta_{fl} \\ \cot\delta \end{bmatrix} = \begin{bmatrix} \frac{r_y + w_{track}/2}{a - r_x} \\ \frac{r_y - w_{track}/2}{a - r_x} \\ \frac{r_y}{a - r_x} \end{bmatrix} = \begin{bmatrix} \frac{r_y + w_{track}/2}{a+b} \\ \frac{r_y - w_{track}/2}{a+b} \\ \frac{r_y}{a+b}. \end{bmatrix} \quad (43)$$

This results in the following identities,

$$\cot\delta_{fr} - \cot\delta = \frac{w_{track}/2}{a+b} \quad (44)$$

$$\cot\delta_{fr} - \cot\delta = \frac{-w_{track}/2}{a+b} \quad (45)$$

$$\cot\delta_{fr} - \cot\delta_{fl} = \frac{w_{track}}{a+b}. \quad (46)$$

The driver is assumed to control the wheel turning angles through δ with 44 and 45 and requests a corresponding vehicle turning radius,

$$R = w_{base}\cot\delta. \quad (47)$$

By assuming that the rear wheels are not steerable, we can write the previous car model only in respect to the steer angle δ as,

$$\dot{\mathbf{x}} = A(\delta)\mathbf{x} + B\mathbf{u} \quad (48)$$

$$\mathbf{y} = C(\delta)\mathbf{x}. \quad (49)$$

4) Steady State: The dynamics matrix A has rank 15-1, which means that there is a surface of equilibrium points. Other equilibrium points may be possible, we don't say anything about them, but those belonging to this surface must exist. If we had taken into account the air resistance then the only equilibrium point would be the origin. This is what we call the "coasting" vehicle. The "coasting" vehicle is possible because, so far, no attrition other than the one from the tire-road interaction has been contemplated.

With the aid of MATLAB we were able to define the null space, $\mathcal{N}(A)$, taking into account different rear and front wheel radius r_r, r_f, as the line spanned by the vector $\mathbf{n}$, normalized in respect to the longitudinal speed v_x and parametrized with the steering δ,

$$\mathcal{N}(A) = v_x\mathbf{n}(\delta), \quad (50)$$

$$\mathbf{n}(\delta) = \begin{bmatrix} 0 \\ 0 \\ \frac{a+b+\tan\delta\cdot w_{track}/2}{r_r(a+b)} \\ 0 \\ 0 \\ \frac{a+b-\tan\delta\cdot w_{track}/2}{r_r(a+b)} \\ 0 \\ 0 \\ \frac{\sqrt{\left((a+b)\cos\delta + \frac{w_{track}}{2}\sin\delta\right)^2 + (a+b)^2\sin^2\delta}}{r_f(a+b)\cos\delta} \\ 0 \\ 0 \\ \frac{\sqrt{\left((a+b)\cos\delta - \frac{w_{track}}{2}\sin\delta\right)^2 + (a+b)^2\sin^2\delta}}{r_f(a+b)\cos\delta} \\ 1 \\ b\frac{\tan\delta}{a+b} \\ \frac{\tan\delta}{a+b} \end{bmatrix}. \quad (51)$$

The null space 51 describes the steady state of the system. It is worth noting that the steady state does not depend on any parameter pertaining to the tire-road interaction, load at each wheel, mass of the vehicle or any other such property. We only require the vehicle dimensions, wheelbase, wheel track, and the tire radius, r_r for the rear tires and r_f for the front tires and the current turning angle δ. Since there is no such dependency, it is not possible to estimate the tire-road interaction if the vehicle is "coasting".

The obtained result for a straight moving vehicle $\mathbf{n}(0)$ is the expected, with the vehicle velocity and each wheel angular velocity depending only on the tire radius. We also derive the relationship between the pairs (ω_z, v_x) and (ω_z, v_y) which shall henceforth be referred as the desired yaw rate and the

lateral stability, respectively. From the vector $\mathbf{n}(\delta)$,

$$\frac{v_x}{\omega_z} = \frac{1}{\tan\delta \ / \ (a+b)} \implies \omega_z = \frac{v_x \tan\delta}{a+b} \tag{52}$$

$$\frac{v_y}{\omega_z} = \frac{b\tan\delta/(a+b)}{\tan\delta/(a+b)} \implies v_y = b \cdot \omega_z \tag{53}$$

we derive the relationships between yaw-rate, longitudinal and lateral velocity.

This is useful in the sense that we can define the desired behaviour, and can also be applied to other problem formulations, such as with the tradicional desired yaw rate equation,

$$\omega_z = \frac{\delta}{a+b+K_u v_x^2} v_x, \tag{54}$$

with the understeer coeficient K_u, which can also be used and tuned to achieve more understeer or oversteer. In this case, the v_x^2 term shoud be either fixed to the current estimated or to the propagated expected value from the system dynamics.

III. Observer/Controller Design

The proposed solution consists on a Model Predictive Controller with an Extended Kalman Filter (EKF) observer. The role of the observer is to estimate the state vector, with an emphasis on the velocity vector. The estimated state $\hat{\mathbf{x}}$ and associated covariance matrix $\hat{P}$ are given to the MPC that will minimize a cost function over the prediction horizon, based on the desired behaviour of the system.

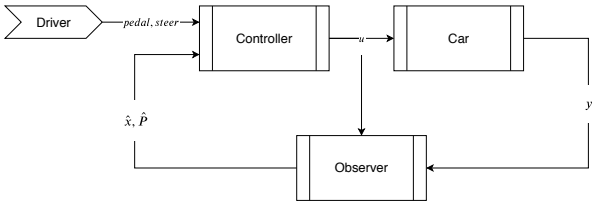

Fig. 8. High level view of the system with the controller and observer. The driver provides a signal, comprised by the pedal and steer. The controller then actuates on the car, given the driver input and the car state estimation from the observer.

A. Observer

The goal of the observer is to provide an accurate estimation of the states, given the plant outputs and the inputs. In order to show if the velocity vector was observable we used an EKF. Should the system be observable, in the simulated conditions, we expect to see a bounded trace of the covariance matrix $trace(\hat{P}_k) < c_{const}, c_{const} > 0$.

Taking the discrete system, we consider that,

$$x_{k+1} = A_k \cdot x_k + B_k \cdot u + w_k \text{ with } w_k \sim N(0, Q) \tag{55}$$

$$y_k = C_k \cdot x_k + v_k \text{ with } v_k \sim N(0, R). \tag{56}$$

The estimation is done through two steps. First we predict what we expect to see. And then, based on the error, we update our estimation.

For the prediction step we take the previous estimation $k-1$, and use he previously linearised model $A_{k-1|k-1}$ to estimate the new state. We use that new estimation to derive a new linearization $A_{k|k-1}$ and calculate the corresponding estimation covariance $\hat{P}_{k|k-1}$.

$$\hat{x}_{k|k-1} = A_{k-1|k-1} \cdot \hat{x}_{k-1|k-1} + B_{k-1|k-1} \cdot u_k \tag{57}$$

$$\hat{P}_{k|k-1} = A_{k|k-1} \cdot \hat{P}_{k-1|k-1} \cdot A_{k|k-1}^T + Q \tag{58}$$

Then we use the error between the measured outputs y_k and the expected outputs to update our estimation through the optimal Kalman gain K_k,

$$e_k = y_k - C_{k|k-1} \cdot \hat{x}_{k|k-1} \tag{59}$$

$$S_k = C_{k|k-1} \cdot P_{k|k-1} \cdot C_{k|k-1}^T + R \tag{60}$$

$$K_k = P_{k|k-1} \cdot C_{k|k-1}^T \cdot S_k^{-1} \tag{61}$$

$$\hat{x}_{k|k} = x_{k|k-1} + K_k \cdot e_k \tag{62}$$

$$\hat{P}_{k|k} = (I - K_k \cdot C_{k|k}) \cdot \hat{P}_{k|k-1}, \tag{63}$$

and make new linearizations $A_{k|k}$ and $C_{k|k}$.

Outside of the observer problem we say that $\hat{x}_k$ is the state estimation at time k and, similarly, that $\hat{P}_k$ is the corresponding covariance matrix. Similarly A_k and C_k correspond to the linearizations.

It is worth noting that proper choice of the expected process noise covariance Q can help with some of the unmodelled dynamics and other disturbances. The sensor noise covariance R must also be adjusted according to the sensors accuracy and noise.

B. Controller

The controller used here is a Model Predictive Controller. Implied with this is an optimization problem that must be solved in real-time. To that effect we selected the KWIK algorithm [48]. The KWIK algorithm solves quadratic programming (QP) problems with linear inequality constraints. Some of our constraints are quadratic but can be approximated by linear constraints. In this section we cover the problem definition, the state and input constraints, as well as an alternate cost function with soft constraints, should some constraints prove to be infeasible for a particular horizon.

1) Model Predictive Controller: MPC is a control strategy under the optimal control umbrella. First developed in the petrochemical industry for process control it has also spread to other areas. It has a strong theoretical basis and its stability, optimality and robustness properties are well known. It is also popular due to it's ability to take into account several constraints, such as in the context of this thesis.

The proposed solution is to transfer the control problem into an optimization problem and solve it through quadratic programming (QP) with a quadratic cost function. This problem is then numerically solved with the KWIK algorithm [48]. Given the discrete piecewise linear system, solve the optimization problem over an horizon window with N timesteps of T_s duration each, with Q and R weight matrices being at least semi-positive definite. Here we will consider only linear constrains, A_u for the inputs and A_x for the state constraints, with the corresponding constraints vectors b_u and

b_x. For a time instance m and N k steps, the problem to be solved is to find the inputs $\mathbf{u}_m$ that minimize,

$$\min_{\mathbf{u}_m} J(\mathbf{u}_m) = \sum_{k=1}^{N} x_{m,k}^T \cdot Q \cdot x_{m,k} + u_{m,k}^T \cdot R \cdot u_{m,k} \tag{64}$$

s.t.

$$\begin{aligned} x_{k+1} &= A_k \cdot x_k + B \cdot u_{k+1} \\ A_u \cdot \mathbf{u}_m &\geq b_u \\ A_x \cdot \mathbf{x}_m &\geq b_x \\ \mathbf{u}_m &= \begin{bmatrix} u_{m,1}^T, & u_{m,2}^T, & \cdots, & u_{m,k}^T, & \cdots, & u_{m,N}^T \end{bmatrix}^T \\ \mathbf{x}_m &= \begin{bmatrix} x_{m,1}^T, & x_{m,2}^T, & \cdots, & x_{m,k}^T, & \cdots, & x_{m,N}^T \end{bmatrix}^T. \end{aligned}$$

To solve the problem we need to rework the problem formulation. The state can be propagated from the initial state x_0 with the system dynamics and inputs as,

$$x_{m,1} = A_0 x_0 + B u_{m,1} \tag{65}$$

$$x_{m,2} = A_1 A_0 x_0 + A_1 B u_{m,1} + B u_{m,2} \tag{66}$$

thus,

$$\mathbf{x}_m = \mathcal{M} x_0 + \mathcal{C} \mathbf{u}_m, \tag{67}$$

with the auxiliary matrices $\mathcal{C}$

$$\mathcal{C} = \begin{bmatrix} B, & 0, & & \ddots & & 0 \\ A_1 B, & B, & 0, & & \ddots & \vdots \\ A_2 A_1 B, & A_1 B, & B, & 0, & & \vdots \\ \vdots & \vdots & \vdots & \vdots & 0 & \vdots \\ (\Pi_{i=N}^{1} A_i) B, & (\Pi_{i=N-1}^{1} A_i) B, & \cdots, & A_2 A_1 B, & A_1 B, & B \end{bmatrix}, \tag{68}$$

and $\mathcal{M}$

$$\mathcal{M} = \begin{bmatrix} A_0 \\ A_1 A_0 \\ A_2 A_1 A_0 \\ \vdots \\ \Pi_{i=N-1}^{0} A_i \end{bmatrix} \tag{69}$$

which allows us to write the the state constraints as inputs constraints,

$$A_x \mathbf{x}_m \geq b_x \tag{70}$$

$$A_x \mathcal{M} x_0 + A_x \mathcal{C} \mathbf{u}_m \geq b_x \tag{71}$$

$$A_x \mathcal{C} \mathbf{u}_m \geq b_x - A_x \mathcal{M} x_0 \tag{72}$$

and adding the previous input constraints we arrive at the more compact form,

$$A_c \mathbf{u}_m \geq b_c \tag{73}$$

$$A_c = \begin{bmatrix} A_x \mathcal{C} \\ A_u \end{bmatrix} \tag{74}$$

$$b_c = \begin{bmatrix} b_x - A_x \mathcal{M} x_0 \\ b_u \end{bmatrix}. \tag{75}$$

We then rewrite the problem,

$$\min_{\mathbf{u}_m} J = \mathbf{u}_m^T H \mathbf{u}_m + 2 \cdot (F \cdot x_0)^T \mathbf{u}_m \tag{76}$$

s.t.

$$\begin{aligned} A_c \mathbf{u} &\geq b_c \\ H &= \mathcal{C}^T Q \mathcal{C} + R \qquad (77) \\ F &= \mathcal{C}^T Q \mathcal{M}, \qquad (78) \end{aligned}$$

which can be solved with the KWIK algorithm [48] if the Hessian matrix H is positive definite $H \succ 0$ and Hermitian $H = H^H$.

Lastly, taking into account that if the car is at rest $x_0 = 0$ and if $H \succeq 0$, then the only possible solution is $\mathbf{u}_m = 0$. To address this, when x_0 is small, it is set to some other slightly higher value. There is a range of values for transitioning, both from rest - driving, and to rest - braking.

2) Input Constraints: The input constraints have to do with the engine curve and the overall available power. We assume that the electric engine will be functioning as an engine, while accelerating, or as a brake, consuming power to brake and not as a generator, consuming mechanical power and generating electric power. However, this section can be revisited for a more in depth power management. We feel that the example provided here is enough for a proof of concept. We could also factor in some constraint/cost to reduce uneven engine wear, like the one proposed in [27] and/or to take into account heat generation.

For the engine curve, we assume that there is some maximum and negative torque, and power constraints when braking and accelerating that define the engine curve. Other engine curves can be considered. The maximum driving and braking torque constraint is trivial to enforce over the horizon, and is considered in the input constraints. For the power constraint we can write it by propagating the wheel speed state and multiplying it by the input torque,

$$P_{engine}^{i} = \omega^i \cdot u^i, \tag{79}$$

with e_s as the wheel speed selector matrix, such that,

$$\mathbf{P}_{engine_m}^{rr,rl,fr,fl} = \text{diag}(\mathbf{u}_m) \cdot (e_s \mathcal{M} x_0 + e_s \mathcal{C} \mathbf{u}_m), \tag{80}$$

we arrive at a quadratic constraint in respect to $\mathbf{u}_m$. This can be avoided if we assume that, besides the one directly connected, the contribution from one engine to some other wheel is negligible. Which amounts to say that the product $e_s \mathcal{C}$ can be approximated through a diagonal matrix. This decouples the problem into constraints to be satisfied by each engine i, since the power at each engine can be approximated by,

$$P_{engine_{m,k}}^{i} = u_{m,k}^{i} \cdot m_{aux} + {u_{m,k}^{i}}^2 \cdot c_{aux}, \tag{81}$$

with m_{aux} and c_{aux} as the corresponding entries of $e_s^i \cdot \mathcal{M} \cdot x_0$ and $e_s^i \cdot \mathcal{C}$. With this, we can solve

$$P_{engine_{m,k}}^{i} \leq \text{max driving/braking engine power}, \tag{82}$$

in respect to the input torque $u_{m,k}^i$ and find the equivalent driving/braking torque constraint as a linear inequality constraint, such that the local power constraints can be written as

$$\mathbf{u}_m \geq b_{\text{equivalent engine torque constraint}}. \tag{83}$$

The equivalent engine torque constraint can be determined by finding the roots of equation 81.

For the overall available power, the previous approximation is not as useful. But we can propagate the wheel turning speed across the horizon with only the autonomous system dynamics

and the previous input solution, getting ${}^*\omega^i_{m,k}$ from $\mathcal{M}x_0 + \mathcal{C}\mathbf{u}_{m-1}$, and say that the power generated at each wheel is approximately given by 79. We then say that the total power consumption must be less than a given limit,

$$P_{\text{total}_{m,k}} \approx \sum_{i}^{rr,rl,fr,fl} {}^*\omega^i_{m,k} \cdot u^i_{m,k}, \tag{84}$$

and use it to make a linear inequality constraint in respect to the inputs.

All of the above was also used to do the braking power constraints, both local and global.

3) State Constraints: The state constraints ensure that there are tip-over safeguards and that the wheel slip ratio does not exceed a predetermined value. The tip-over safeguards can be made to enforce a minimum load at each tire or to limit the lateral g forces. The wheel slip constraint can be turned into a linear constraint if we rewrite 1 into,

$$v^i_x(k+1) - \omega r = 0, \tag{85}$$

with v^i_x as the longitudinal speed at a tire i in the tire frame. Which results in the following linear constraints,

$$v^i_x(1+k^+) - \omega^i r \geq 0 \tag{86}$$

$$v^i_x(1-k^-) + \omega^i r \geq 0. \tag{87}$$

The velocities at each tire can then be mapped into velocities at the centre of mass with the linear transformation 27, thus ensuring we can have this constraint as a linear constraint in our optimization problem 64,

$$\begin{bmatrix} -r & \begin{bmatrix}(1+k^+) & 0\\ (1-k^-) & 0\end{bmatrix} \end{bmatrix} \begin{bmatrix} \cos\delta & \sin\delta & r_x\sin\delta - r_y\cos\delta \\ -\sin\delta & \cos\delta & r_x\cos\delta + r_y\sin\delta \end{bmatrix} \begin{bmatrix} \omega^i \\ v_x \\ v_y \\ \omega_z \end{bmatrix} \geq 0 \tag{88}$$

$$\implies \begin{bmatrix} -r & (1+k^+)\cos\delta & (1+k^+)\sin\delta & (1+k^+)(r_x\sin\delta - r_y\cos\delta) \\ r & (1-k^-)\cos\delta & (1-k^-)\sin\delta & (1-k^-)(r_x\sin\delta - r_y\cos\delta) \end{bmatrix} \begin{bmatrix} \omega^i \\ v_x \\ v_y \\ \omega_z \end{bmatrix} \geq 0. \tag{89}$$

For the tip-over problem we can define a limit for the g forces. This means that if a turning radius is requested that can't satisfy this constraint at the initial velocity, the controller will brake the car in such a way that it does the tightest turn with, at most, the specified g force until the requested turning radius is achieved. It will then only expend energy in maintaining that velocity. Similarly, the controller will allow the car to accelerate until the maximum gforce is achieved.

The lateral g forces are considered to be only due to the centrifugal force, which is also responsible for the lateral load transfer, disregarding the contribution from $\dot{v}_y$,

$$g_{force_y} = \text{sign}(\omega_z)\frac{v_x \cdot \omega_z}{g} \tag{90}$$

Any constraint done here in respect to both the longitudinal velocity and the yaw rate results in a non-linear constraint. Since we can directly measure the yaw rate, the approach taken here was to propagate the longitudinal velocity and use that value has a constant,

$$\frac{g \cdot g_{force\ limit_y}}{{}^*v_x} \geq |\omega_z| \tag{91}$$

which can be turned into two linear constraints, one for the lower bound and another for the upper bound of ω_z, for each time step.

The tip-over prevention can also be ensured by placing steering constraints on the input steer from the driver and limiting the maximum steer angle as in stated by Kang [28]. Or by making constraint similar to the g force constraint, based on the minimum acceptable normal load at each tire.

4) Cost Function: According to the system dynamics, the cost function must minimize the lateral stabilization error and ensure the yaw rate - linear velocity relationship. At thrust, we want a compromise between the highest longitudinal speed at the end of the horizon $v_{x|N}$ and the minimum error during the horizon. With some positive weight factors ρ we devised the following cost function,

$$\min_{\mathbf{u}_m} J = -\rho_{v_x} v^2_{x,N} + \sum_{k=1}^{N} \left[\rho_{\omega_z} \left(\omega_{z,k} - \frac{v_{x,k}\tan\delta}{a+b} \right)^2 + \rho_l (v_{y,k} - b\omega_{z,k} \tag{92}$$

(93)

that happens to result in a symmetric positive definite matrix H 76. Should H not be positive definite at some point, it can be reconstructed to provide a convex hull by decomposing it and enforcing positive eigenvalues. In practice, only least energetic component was negative. For the most part H is at least semi-positive definite $H \succeq 0$. Whether or not H is full rank is tied to whether or not the system is over-actuated. In those cases we can't ensure that the solution is the most optimum solution, in the sense of optimum control.

Should the MPC problem be infeasible, we need to known why. One possibility is when the slip constraints for a given wheel can't be met. In such a case a quadratic cost J_{slip} for those wheels is added to the cost function in order to bring it back to feasibility,

$$J_{slip} = \rho_{slip} \sum \left(v^i_x - \omega^i r \right)^2 \tag{94}$$

with ρ_{slip} as a weight and the sum being only about those wheels.

The other possibility for an infeasible problem is if the g force can't be within bounds over the horizon. In which case we also add a very high quadratic cost to the yaw rate ω_z in order to reduce the g force.

With this we can ensure that even when the problem is infeasible, we can move towards a feasible operation point without dismissing the original problem formulation.

IV. Verification and Validation

The verification and validation of the model was done through the state estimations from the EKF on a run with the FST09e. The car had two engines on a rear wheel configuration, and only those angular velocities were available, since those measurements are tied to the engines. Figure 9 shows the result of the integration of the velocity and yaw rate estimations. The line colour is such that green means that the instant center of rotation is on the line that passes through the rear axle, red that is bellow it, and blue that it is above.

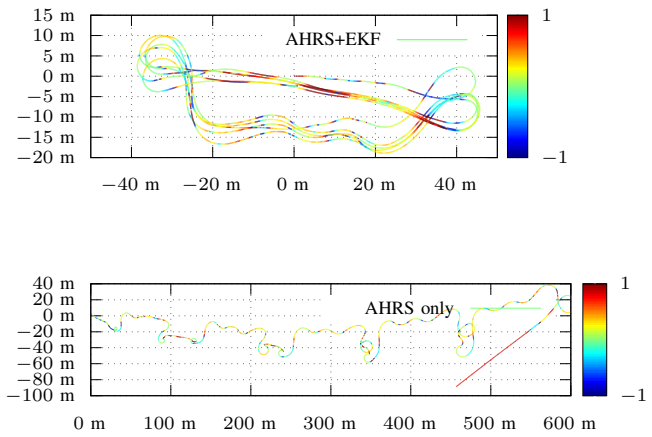

Fig. 9. Trajectory estimation by integrating the velocity and yaw rate estimations from the EKF at 100Hz. The car starts at the origin and first moves along the positive x axis, to the right. The line color shows racio of the sideslip angle at the rear axle and at the cg $\frac{\beta_r}{\beta_c}$.

Ideally we want the sideslip angle at the rear axle β_r to be 0.

As it can be seen, even though we don't have data about all the wheels, only the driving ones, and in spite of parameter uncertainty - many of the parameters could not be validated, the estimation shows a trajectory that has the shape of the test track and it "closes the circle" of more than 600m in a ≈ 3 min test run on a vehicle that at some points reached almost 2g of lateral force. While this is a qualitative measure, the comparison with the sensor data serves to show how much of an improvement the estimation made.

V. Conclusions

Looking at the work developed, the results, and taking into account what we set up to do, we can say that we met all the proposed objectives. The only thing we could not verify was the performance of the controller in the car, although the observer alone is sufficient to justify this and further work. Should the attitude estimations be correct, in spite of the parameter uncertainties, then we managed to do with a common sensor and some current measurements, what dedicated and expensive sensors do, and we could implement this observer into virtually any electric car.

We managed to do a robust controller, agnostic to the number of driving wheels, capable of enforcing power constraints, attitude constraints, achieving desired yaw rates and slip ratios, tunable and customizable for other needs and objectives.

After the conclusion of this work, we believe that an online parameter estimation for the tire/road interaction and some car parameters should be developed and the state estimation problem should be incorporated into the model predictive controller since the observation and control problems are not completely separable. The solver should also be independently implemented in order to be more efficient and natively support the switching of hard constraints into soft constraints. In line with this, more work on the observability and detectability of the system should be done.

Another point that could be better explored is how the pedal interacts with the controller. Currently the pedal is assumed to control the total available power, but also having it as a factor in the velocity weight of the MPC might be a better approach, or even in the slip ratio limit.

An electric engine state space model, as long as it is linear, could also be incorporated into the controller, thus changing the problem from a torque perspective into a current perspective. Should the resulting model also be observable, this could be a factor for the engine temperature and wear estimation, that could be used as weights in the controller, thus providing the foundation for cooling strategies, even wear and temperature control by placing weights on the actuation, based on these measures.

Lastly, the suspension model should be incorporated in order to have better normal load estimations and, consequently tire slip estimations. And maybe in the future, we could also develop active suspension models that could further improve handling.

Even the tire model, could be improved by taking into account all the non linearities that were not fully explored in this work, such as conicity and temperature to name a few.

But all of this can only be accomplished with proper state estimation and known vehicle dynamics. We hope that more work can be done as a result of this thesis and problem formulation.

References

[1] Hasan Alipour, Mehran Sabahi, and Mohammad Bagher Bannae Sharifian. "Lateral stabilization of a four wheel independent drive electric vehicle on slippery roads". In: *Mechatronics* 30 (2015), pp. 275–285. ISSN: 09574158. DOI: 10.1016/j.mechatronics.2014.08.006. URL: http://dx.doi.org/10.1016/j.mechatronics.2014.08.006.

[2] Pierre Apkarian, Pascal Gahinet, and Greg Becker. "Self-scheduled H∞ control of linear parameter-varying systems: a design example". In: *Automatica* 31.9 (1995), pp. 1251–1261. ISSN: 00051098. DOI: 10.1016/0005-1098(95)00038-X.

[3] G Arun. "Fractional PID and Sliding-Mode-Controller for Active Vehicle Suspension System". In: (2015), pp. 1428–1434.

[4] Jakob Bechtoff, Lars Koenig, and Rolf Isermann. "Cornering Stiffness and Sideslip Angle Estimation for Integrated Vehicle Dynamics Control". In: *IFAC-PapersOnLine* 49.11 (2016), pp. 297–304. ISSN: 24058963. DOI: 10.1016/j.ifacol.2016.08.045. URL: http://dx.doi.org/10.1016/j.ifacol.2016.08.045.

[5] Thomas Besselmann, Johan Löfberg, and Manfred Morari. "Explicit MPC for LPV systems: Stability and optimality". In: *IEEE Transactions on Automatic Control* 57.9 (2012), pp. 2322–2332. ISSN: 00189286. DOI: 10.1109/TAC.2012.2187400.

[6] Stephen Boyd et al. "Distributed optimization and statistical learning via the alternating direction method of multipliers". In: *Foundations and Trends in Machine Learning* 3.1 (2010), pp. 1–122. ISSN: 19358237. DOI: 10.1561/2200000016.

[7] C. Canudas de Wit et al. “A new model for control of systems with friction”. In: *IEEE Transactions on Automatic Control* 40.3 (Mar. 1995), pp. 419–425. ISSN: 00189286. DOI: 10.1109/9.376053. URL: http://ieeexplore.ieee.org/document/376053/.

[8] Yu Cao et al. “Straight Running Stability Control Based on Optimal Torque Distribution for a Four in-wheel Motor Drive Electric Vehicle”. In: *Energy Procedia* 105 (2017), pp. 2825–2830. ISSN: 18766102. DOI: 10.1016/j.egypro.2017.03.616.

[9] Christoforos Chatzikomis et al. “Comparison of Path Tracking and Torque-Vectoring Controllers for Autonomous Electric Vehicles”. In: *IEEE Transactions on Intelligent Vehicles* 3.4 (2018), pp. 559–570. ISSN: 2379-8858. DOI: 10.1109/tiv.2018.2874529.

[10] David A. Crolla and Dongpu Cao. “The impact of hybrid and electric powertrains on vehicle dynamics, control systems and energy regeneration”. In: *Vehicle System Dynamics* 50.sup1 (Jan. 2012), pp. 95–109. ISSN: 0042-3114. DOI: 10.1080/00423114.2012.676651. URL: http://www.tandfonline.com/doi/abs/10.1080/00423114.2012.676651.

[11] Joško Deur. “Modeling and Analysis of Longitudinal Tire Dynamics Based on the Lugre Friction Model”. In: *IFAC Proceedings Volumes* 34.1 (2001), pp. 91–96. ISSN: 14746670. DOI: 10.1016/s1474-6670(17)34383-5.

[12] Josko Deur, Jahan Asgari, and Davor Hrovat. “A 3D brush-type dynamic tire friction model”. In: *Vehicle System Dynamics* 42.3 (2004), pp. 133–173. ISSN: 00423114. DOI: 10.1080/00423110412331282887.

[13] Joško Deur et al. “Extensions of the LuGre tyre friction model related to variable slip speed along the contact patch length”. In: *Vehicle System Dynamics* 43.SUPPL. (Jan. 2005), pp. 508–524. ISSN: 00423114. DOI: 10.1080/00423110500229808. URL: http://www.tandfonline.com/doi/abs/10.1080/00423110500229808.

[14] S.V. Drakunov. “Sliding-mode observers based on equivalent control method”. In: 9 (2005), pp. 2368–2369. DOI: 10.1109/cdc.1992.371368.

[15] K. El Majdoub et al. “Vehicle longitudinal motion modeling for nonlinear control”. In: *Control Engineering Practice* 20.1 (2012), pp. 69–81. ISSN: 09670661. DOI: 10.1016/j.conengprac.2011.09.005.

[16] Gurkan Erdogan. “Why Tires are important for Vehicle Control Systems ?” In: (2009), pp. 2–28.

[17] Marcello Farina, Giancarlo Ferrari-Trecate, and Riccardo Scattolini. “Distributed Moving Horizon Estimation for Linear Constrained Systems”. In: *IEEE Transactions on Automatic Control* 55.11 (Nov. 2010), pp. 2462–2475. ISSN: 0018-9286. DOI: 10.1109/TAC.2010.2046058. URL: http://doi.wiley.com/10.1002/rnc.1676%20http://ieeexplore.ieee.org/document/5437313/.

[18] Yuan Feng et al. “Torque Vectoring Control for Distributed Drive Electric Vehicle Based on State Variable Feedback”. In: *SAE International Journal of Passenger Cars - Electronic and Electrical Systems* 7.2 (2014), pp. 328–336. ISSN: 19464622. DOI: 10.4271/2014-01-0155.

[19] Michel Fliess, Cédric Join, and Hebertt Sira-Ramírez. “Non-linear estimation is easy”. In: *International Journal of Modelling, Identification and Control* 4.1 (2008), pp. 12–27. ISSN: 17466180. DOI: 10.1504/IJMIC.2008.020996. arXiv: 0710.4486.

[20] Reiner Folke et al. “Torque vectoring a new level of freedom for electric vehicles”. In: *ATZ worldwide* 112.6 (2010), pp. 8–12. DOI: 10.1007/bf03225125.

[21] Jyotishman Ghosh, Andrea Tonoli, and Nicola Amati. “A Torque Vectoring Strategy for Improving the Performance of a Rear Wheel Drive Electric Vehicle”. In: *2015 IEEE Vehicle Power and Propulsion Conference, VPPC 2015 - Proceedings* (2015). DOI: 10.1109/VPPC.2015.7352887.

[22] Supratim Ghosh and Justin Ruths. “On structural controllability of a class of bilinear systems”. In: *Proceedings of the IEEE Conference on Decision and Control* 2015-Febru.February (2014), pp. 3137–3142. ISSN: 07431546. DOI: 10.1109/CDC.2014.7039873.

[23] Alf J. Isaksson et al. “Using horizon estimation and nonlinear optimization for grey-box identification”. In: *Journal of Process Control* 30 (2015), pp. 69–79. ISSN: 09591524. DOI: 10.1016/j.jprocont.2014.12.008. URL: http://dx.doi.org/10.1016/j.jprocont.2014.12.008.

[24] Valentin Ivanov et al. “Electric vehicles with individually controlled on-board motors: Revisiting the ABS design”. In: *Proceedings - 2015 IEEE International Conference on Mechatronics, ICM 2015*. 2015, pp. 323–328. ISBN: 9781479936335. DOI: 10.1109/ICMECH.2015.7083996.

[25] Reza N Jazar. *Vehicle Dynamics*. Cham: Springer International Publishing, 2017. ISBN: 978-3-319-53440-4. DOI: 10.1007/978-3-319-53441-1. URL: http://link.springer.com/10.1007/978-3-319-53441-1.

[26] Chi Jin et al. “Vehicle Side Slip Angle Observation with Road Friction Adaptation”. In: *IFAC-PapersOnLine* 50.1 (2017), pp. 3406–3411. ISSN: 24058963. DOI: 10.1016/j.ifacol.2017.08.593. URL: https://doi.org/10.1016/j.ifacol.2017.08.593.

[27] Angelos Kampanakis et al. “A Torque Vectoring Optimal Control Strategy for Combined Vehicle Dynamics Performance Enhancement and Electric Motor Ageing Minimisation”. In: *IFAC-PapersOnLine* 49.11 (2016), pp. 412–417. ISSN: 24058963. DOI: 10.1016/j.ifacol.2016.08.061. URL: http://dx.doi.org/10.1016/j.ifacol.2016.08.061.

[28] Juyong Kang, Jinho Yoo, and Kyongsu Yi. “Driving Control Algorithm for Maneuverability, Lateral Stability, and Rollover Prevention of 4WD Electric Vehicles With Independently Driven Front and Rear Wheels”. In: *IEEE Transactions on Vehicular Technology* 60.7 (Sept. 2011), pp. 2987–3001. ISSN: 0018-9545. DOI: 10.1109/TVT.2011.2155105. URL: http://ieeexplore.ieee.org/document/5770244/.

[29] Dhanaraja Kasinathan et al. “An Optimal Torque Vectoring Control for Vehicle Applications via Real-Time

Constraints". In: *IEEE Transactions on Vehicular Technology* 65.6 (2016), pp. 4368–4378. ISSN: 00189545. DOI: 10.1109/TVT.2015.2467374.

[30] S. Kaspar et al. "Robust torque vectoring control". In: *IFAC Proceedings Volumes (IFAC-PapersOnline)* 19 (2014), pp. 12023–12028. ISSN: 14746670. DOI: 10.3182/20140824-6-za-1003.02359.

[31] Edward M. Kasprzak and David Gentz. "The formula sae tire test consortium-tire testing and data handling". In: *SAE Technical Papers* (2006). ISSN: 26883627. DOI: 10.4271/2006-01-3606.

[32] Nikolaos Kazantzis and Costas Kravaris. "Nonlinear observer design using Lyapunov's auxiliary theorem". In: *Proceedings of the IEEE Conference on Decision and Control* 5.June 1997 (1997), pp. 4802–4807. ISSN: 01912216. DOI: 10.1016/S0167-6911(98)00017-6.

[33] Matthias Korte et al. "Design of a robust adaptive vehicle observer towards delayed and missing Vehicle Dynamics sensor signals by usage of Markov Chains". In: *Proceedings of the American Control Conference* June (2013), pp. 6798–6803. ISSN: 07431619. DOI: 10.1109/acc.2013.6580907.

[34] Arthur J. Krener and Alberto Isidori. "Linearization by output injection and nonlinear observers". In: *Systems and Control Letters* 3.1 (1983), pp. 47–52. ISSN: 01676911. DOI: 10.1016/0167-6911(83)90037-3.

[35] Seung Hi Lee et al. *Slip angle estimation: Development and experimental evaluation*. Vol. 8. PART 1. IFAC, 2013, pp. 286–291. ISBN: 9783902823366. DOI: 10.3182/20130626-3-AU-2035.00071. URL: http://dx.doi.org/10.3182/20130626-3-AU-2035.00071.

[36] Jingliang Li, Yizhai Zhang, and Jingang Yi. "A hybrid physical-dynamic tire/road friction model". In: *Journal of Dynamic Systems, Measurement and Control, Transactions of the ASME* 135.1 (2013). ISSN: 00220434. DOI: 10.1115/1.4006887.

[37] Qian Lu et al. "H∞ loop shaping for the torque-vectoring control of electric vehicles: Theoretical design and experimental assessment". In: *Mechatronics* 35 (2016), pp. 32–43. ISSN: 09574158. DOI: 10.1016/j.mechatronics.2015.12.005. URL: http://dx.doi.org/10.1016/j.mechatronics.2015.12.005.

[38] L. Menini and A. Tornamb?? "Feedback linearization of impulsive nonlinear control systems". In: *AIP Conference Proceedings* 1479.1 (2012), pp. 1447–1449. ISSN: 0094243X. DOI: 10.1063/1.4756433.

[39] Asal Nahidi et al. "Modular integrated longitudinal and lateral vehicle stability control for electric vehicles". In: *Mechatronics* 44 (2017), pp. 60–70. ISSN: 09574158. DOI: 10.1016/j.mechatronics.2017.04.001.

[40] Leonardo de Novellis et al. "Torque vectoring for electric vehicles with individually controlled motors: State-of-the-art and future developments". In: *World Electric Vehicle Journal* 5.2 (2012), pp. 617–628. ISSN: 20326653. DOI: 10.3390/wevj5020617.

[41] Hans B. Pacejka. *Tire and Vehicle Dynamics*. Elsevier, 2006. ISBN: 9780750669184. DOI: 10.1016/B978-0-7506-6918-4.X5000-X. URL: http://www.engineering108.com/Data/Engineering/Automobile/tyre-and-vehicle-dynamics.pdf%20https://linkinghub.elsevier.com/retrieve/pii/B9780750669184X5000X.

[42] Hans B. Pacejka and Egbert Bakker. "THE MAGIC FORMULA TYRE MODEL". In: *Vehicle System Dynamics* 21.sup001 (Jan. 1992), pp. 1–18. ISSN: 0042-3114. DOI: 10.1080/00423119208969994. URL: http://www.tandfonline.com/doi/abs/10.1080/00423119208969994.

[43] Alberto Parra et al. "Intelligent Torque Vectoring Approach for Electric Vehicles with Per-Wheel Motors". In: *Complexity* 2018 (2018). ISSN: 10990526. DOI: 10.1155/2018/7030184.

[44] Karmvir Singh Phogat, Debasish Chatterjee, and Ravi N. Banavar. "A discrete-time Pontryagin maximum principle on matrix Lie groups". In: *Automatica* 97 (2018), pp. 376–391. ISSN: 00051098. DOI: 10.1016/j.automatica.2018.08.026. arXiv: 1612.08022. URL: https://doi.org/10.1016/j.automatica.2018.08.026.

[45] Bingtao Ren et al. "MPC-based yaw stability control in in-wheel-motored EV via active front steering and motor torque distribution". In: *Mechatronics* 38 (2016), pp. 103–114. ISSN: 09574158. DOI: 10.1016/j.mechatronics.2015.10.002. URL: http://dx.doi.org/10.1016/j.mechatronics.2015.10.002.

[46] I. Michael Ross et al. "Riemann-Stieltjes optimal control problems for uncertain dynamic systems". In: *Journal of Guidance, Control, and Dynamics* 38.7 (2015), pp. 1251–1263. ISSN: 07315090. DOI: 10.2514/1.G000505.

[47] Volker Scheuch et al. "A safe Torque Vectoring function for an electric vehicle". In: *World Electric Vehicle Journal* 6.3 (2013), pp. 731–740. ISSN: 20326653. DOI: 10.1109/EVS.2013.6915027.

[48] C. Schmid and L.T. Biegler. "Quadratic programming methods for reduced hessian SQP". In: *Computers & Chemical Engineering* 18.9 (Sept. 1994), pp. 817–832. ISSN: 00981354. DOI: 10.1016/0098-1354(94)E0001-4. URL: https://linkinghub.elsevier.com/retrieve/pii/0098135494E00014.

[49] Zhibin Shuai et al. "Lateral motion control for four-wheel-independent-drive electric vehicles using optimal torque allocation and dynamic message priority scheduling". In: *Control Engineering Practice* 24.1 (2014), pp. 55–66. ISSN: 09670661. DOI: 10.1016/j.conengprac.2013.11.012. URL: http://dx.doi.org/10.1016/j.conengprac.2013.11.012.

[50] Efstathios Siampis, Efstathios Velenis, and Stefano Longo. "Torque Vectoring Model Predictive Control with Velocity Regulation Near the Limits of Handling". In: *Vehicle System Dynamics* (2015), pp. 2553–2558. ISSN: 17445159. DOI: 10.1080/00423114.2015.1064972. URL: http://www.tandfonline.com/doi/pdf/10.1080/00423114.2015.1064972.

[51] J Slotine and W Li. *Applied Nonlinear Control*. 1990. ISBN: 0130408905.

[52] Jacob Svendenius and Magnus Gäfvert. "A semi-empirical dynamic tire model for combined-slip forces".

In: *Vehicle System Dynamics* 44.2 (2006), pp. 189–208. ISSN: 00423114. DOI: 10.1080/00423110500385659.

[53] Discrete-time Control Systems. "Discretization of Continuous-Time Systems". In: *Journal of The Society of Instrument and Control Engineers* 32.2 (1993), pp. 120–127. ISSN: 1883-8170. DOI: 10 . 11499 / sicejl1962.32.120.

[54] Zhiqiang Tang. "Modeling and Estimation of Dynamic Tire Properties". In: *Electrical Engineering* 54.1 (2010), pp. 13–34. URL: http : / / www . vehicular . isy . liu . se / Publications/MSc/09%7B%5C_%7DEX%7B%5C_%7D4227%7B%5C_%7DJL.pdf.

[55] B. Tibken and E. P. Hofer. "Systematic observer design for bilinear systems". In: *Proceedings - IEEE International Symposium on Circuits and Systems* 3.9 (1989), pp. 1611–1616. ISSN: 02714310. DOI: 10.1109/iscas.1989.100671.

[56] Panagiotis Tsiotras, Efstathios Velenis, and Michel Sorine. "A LuGre tire friction model with exact aggregate dynamics". In: *Proceedings of the American Control Conference* 2 (2004), pp. 1457–1462. ISSN: 07431619. DOI: 10.1109/ACC.2004.182988.

[57] J. Velazquez Alcantar and F. Assadian. "Vehicle dynamics control of an electric-all-wheel-drive hybrid electric vehicle using tyre force optimisation and allocation". In: *Vehicle System Dynamics* 57.12 (Dec. 2019), pp. 1897–1923. ISSN: 0042-3114. DOI: 10.1080/00423114.2019.1585556. URL: https://www.tandfonline.com/doi/full/10.1080/00423114.2019.1585556.

[58] E. Velenis et al. "Dynamic tyre friction models for combined longitudinal and lateral vehicle motion". In: *Vehicle System Dynamics* 43.1 (Jan. 2005), pp. 3–29. ISSN: 0042-3114. DOI: 10 . 1080 / 00423110412331290464. URL: http://www.tandfonline.com/doi/abs/10.1080/00423110412331290464.

[59] X. D. Wu et al. "Parameter identification for a LuGre model based on steady-state tire conditions". In: *International Journal of Automotive Technology* 12.5 (Oct. 2011), pp. 671–677. ISSN: 1229-9138. DOI: 10.1007/s12239-011-0078-9. URL: http://link.springer.com/10.1007/s12239-011-0078-9.

[60] M. Zeitz. "The extended Luenberger observer for nonlinear systems". In: *Systems and Control Letters* 9.2 (1987), pp. 149–156. ISSN: 01676911. DOI: 10.1016/0167-6911(87)90021-1.